ChemComm

Accepted Manuscript

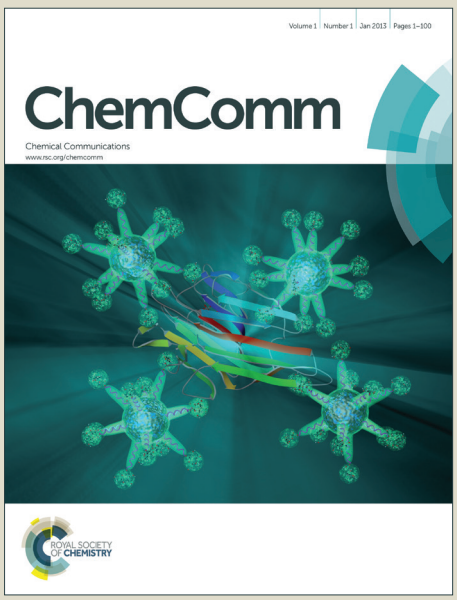

ROYAL SOCIETY OF CHEMISTRY

www.rsc.org/chemcomm

Cite this: DOI: 10.1039/c0xx00000x

www.rsc.org/xxxxxx

ARTICLE TYPE

Organic alloys of room temperature liquids thiophenol and selenophenol

Sajesh P. Thomas, R. Sathishkumar and T. N. Guru Row*

Received (in XXX, XXX) Xth XXXXXXXXX 20XX, Accepted Xth XXXXXXXXX 20XX
DOI: 10.1039/b000000x

The first examples of organic alloys of two room temperature liquids, obtained and characterized via *in situ* cryo-crystallography, are presented. Thiophenol and selenophenol, which exhibit isostructurality and similar modes of S···S and Se···Se homo-chalcogen interactions along with weak and rare S–H···S and Se–H···Se hydrogen bonds, are shown to form solid solutions exhibiting Veggard's law-like trends.

Supramolecular chemistry of multi-component organic crystals is one of the major focuses of crystal engineering research.[1] The plethora of co-crystals that have been synthesized and the structurally analyzed in the past two decades have provided insights into various supramolecular recognition units. Besides, co-crystals have found a variety of applications in pharmaceutical chemistry[2] and material science.[3] Many of these multi-component systems are generated utilizing 'supramolecular synthons',[4] which are based on intermolecular binding affinity between different functional groups in organic molecules. While co-crystals exhibit definite stoichiometry of components, there are some examples of solids known as organic alloys/solid solutions for which this stoichiometry can be varied. Organic alloys of functional organic solids are of special significance,[5] as they provide a means to tune the properties of the material.[6] Though variable stoichiometries are common for inorganic materials such as metal alloys and minerals, there are only a few examples for alloys formed by organic molecules. The similar sized inorganic components such as metal ions with strong and similar ionic bonding directionality can facilitate the formation of alloys with substituted metal ions.[7] In contrast, the diversity in shapes and structural complexity in organic molecules make the design of organic alloys a hard task. The known examples of organic alloys or solid solutions may be classified into two types; (i) structures for which the component molecules are very similar in size,[8] shape[9], and interaction propensity[10], and (ii) those which form host-guest type crystal structures[11] with porous frameworks[12] that allow variable stoichiometry of the guest molecules. For the known examples of solid solutions at least one of the molecular components is a room temperature-solid, and to our knowledge there are no examples of organic alloys formed by two room-temperature liquids. Herein we present the crystal structures of the room-temperature liquids thiophenol and selenophenol (benzeneselenol) and those of their solid solutions. These 'organic alloy' phases were obtained and characterized by i*n situ* cryocrystallographic technique. The crystal structures of the compounds thiophenol and selenophenol were investigated as a part of our research on weak intermolecular interactions. Non-covalent interactions other than classical hydrogen bonds, such as halogen bonding,[13] chalcogen bonding,[14-16] pnicogen bonding,[17] carbon bonding,[18] etc. are of special interest as their implications

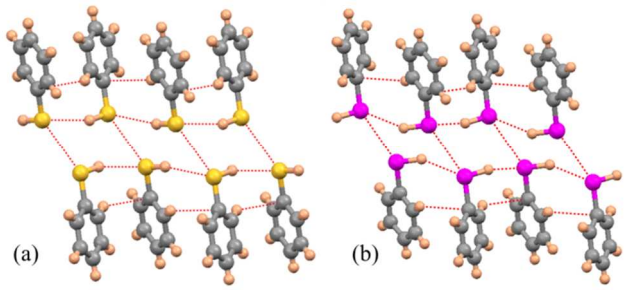

Fig 1. (a) S–H···S hydrogen bond chain formation in thiophenol, supported by S···S interactions and (b) corresponding Se–H···Se hydrogen bond chains and Se···Se interactions in selenophenol (C-grey, H-almond brown, S-yellow and Se-magenta)

in crystal packing have not been clearly understood. In addition, probing liquids using i*n situ* cryocrystallographic technique provides the prospects of understanding the 'pure' interaction preferences of molecules during the process of supramolecular aggregation, unaffected by solvent effects. In the present study, thiophenol and selenophenol have been examined in order to compare the intermolecular interactions present in their crystal structures with those in the crystal forms of phenol. The weak and rare S–H···S and Se–H···Se hydrogen bonds, along with S···S and Se···Se chalcogen bonding interactions have been compared in terms of their strengths and charge density topological features.

The crystal phases of thiophenol (melting point, -15°C) and selenophenol (melting point, -23°C) were grown in Lindemann glass capillaries by slowly cooling the liquids using a nitrogen cryostream (See ESI for details). *In situ* cryocrystallographic study shows that both thiophenol and selenophenol crystallize in the orthorhombic space group *Pnab* with *Z*=8. These structures exhibit similarity to the high pressure form of phenol. Phenol is known to exhibit two polymorphs; an ambient pressure polymorph[19] stabilized by helical O–H···O hydrogen bond chains and a high pressure form[20] characterized by zig-zag antiparallel O–H···O hydrogen bond chains. Crystal structure analysis shows that thiophenol and selenophenol are isostructural to each other (Fig 1, Table 1) and different from the ambient pressure form of phenol. The crystal packing in thiophenol is supported by antiparallel S–H···S hydrogen bond chains (Figure 2a) whereas in selenophenol it is stabilized by similar Se–H···Se hydrogen bond chains (Figure 2b). In addition, in both the structures there exist C–H···π interactions that support these molecular chains. Interestingly, thiophenol exhibits a S···S chalcogen bonding of interaction distance 3.580(2) Å. Similarly, selenopheniol exhibits a Se···Se chalcogen bonding of interaction distance 3.756(2) Å. The homo-chalcogen interactions are the main intermolecular

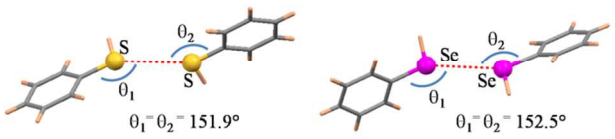

Fig 2. The homo-chalcogen interactions in thiophenol and selenophenol highlighting the ∠C–S···S angle.

features that distinguish these crystal structures from that of phenol. It may be noted that the S···S interaction geometry in thiophenol has a ∠C–S···S angle of 151.9°, and Se···Se interaction in selenophenol has a ∠C–Se···Se angle of 152.5° akin to those found in type I halogen···halogen contacts.[21] A survey on these homo-chalcogen interactions in Cambridge Structural Database (CSD version 5.36 February 2015) results in 7112 crystal structure entries having S···S contact distances less than 3.6 Å, the sum of van der Waals radii. The mean S···S contact distance was found to be 3.471 Å. Similarly, 1049 structures were found to exhibit Se···Se homochalcogen interactions with a mean contact distance of 3.605 Å (the sum of van der Waals radii being 3.8 Å). Hence, the observed contacts in thiophenol and selenophenol represent only weak or borderline cases of homo-chalcogen interactions despite the absence of any strong intermolecular hydrogen bonds in those structures. A search for the Se···S hetero-chalcogen interactions resulted in 253 hits with a mean Se···S contact distance of 3.560 Å. This is particularly interesting, considering the isostructurality of these compounds. Hence, inspired from the observed isostructurality in crystal structures of thiophenol and selenophenol, we made several attempts to grow *in situ* their solid solutions. The liquid samples of thiophenol and selenophenol were mixed thoroughly via sonification, before filling into the capillary. Mixtures of selenophenol: thiophenol with different volume ratios were used for *in situ* crystal growth experiments. Of all the different crystal phases obtained (of sufficient data quality), four solid solution phases with different compositions were distinctly identified. The percentage compositions of selenophenol in these solid solution phases were found to be 5%, 9%, 25% and 43%. These compositions were obtained when mixtures of 1:9, 1:4 and 1:3 ratios were used for the experiment. The compositions were identified based on the site occupancy refinements of S and Se atoms (based on an occupancy free variable, FVAR. For details, see Table S1 in ESI). After several cycles of free occupancy refinements, the percentage composition of selenophenol were approximated to 5%, 9%, 25% and 43% respectively (for details of crystal structure refinement and molecular formulae of alloy phases see ESI). It is interesting to note the variation in cell parameters of the solid solution with the increase in the percentage of selenophenol (Table 1 and Fig 3). Though the variation is not quite linear, the gradual variations in cell parameters loosely mimic the trends observed in inorganic solids (as indicated by Vegard's law).[22] Although similar attempts

Table 1. Crystallographic refinement details of thiophenol, selenophenol and their solid solutions (selenophenol: thiophenol).

Data	Thio-phenol	Seleno-phenol	5: 95 solid solution	9: 91 solid solution	25: 75 solid solution	43: 57 solid solution
Space group	*Pnab*	*Pnab*	*Pnab*	*Pnab*	*Pnab*	*Pnab*
a (Å)	7.191(1)	7.329(4)	7.191 (1)	7.193(2)	7.211(1)	7.262(2)
b (Å)	11.464(2)	11.226(5)	11.445(1)	11.425(3)	11.390 (2)	11.371(3)
c (Å)	13.815(2)	14.422(7)	13.854(1)	13.856(4)	13.971(2)	14.155(3)
α (°)	90	90	90	90	90	90
β (°)	90	90	90	90	90	90
γ (°)	90	90	90	90	90	90
Volume (Å^3)	1138.8(3)	1186.6(10)	1140.2(2)	1138.8(5)	1147.4(3)	1168.9(5)
Z	8	8	8	8	8	8

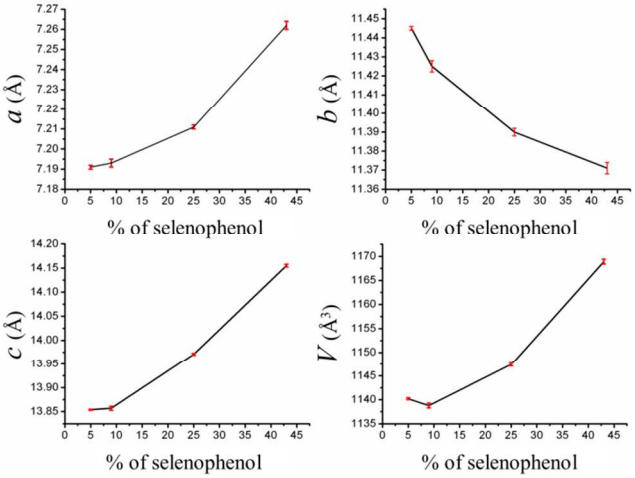

Fig 3. Variations in unit cell parameters and volume with percentage composition of selenophenol in the alloy phases.

were made to generate solid solutions of phenol-thiophenol mixtures and phenol-selenophenol mixtures, they resulted in glassy/amorphous domains. However, the fact that these mixtures did not crystallize as separate crystal domains of individual components is significant, and two possible reasons may be conjectured; (i) due to the formation of hetero-chalcogen bonding such as S···O and Se···O interactions (which are known to form directional supramolecular motifs[14, 23]), and (ii) due to the incompatibility of the strong and short O–H···O hydrogen bonds with the weak S–H···S and Se–H···Se hydrogen bonds.

Further, the structural features that lead to isostructurality of thiophenol and selenophenol have been quantitatively examined. Firstly, Hirshfeld fingerprint breakdown analysis[24] shows that the proportion of H···C dominates with 31.9% in thiophenol and 30.5% in selenophenol. H···S and H···Se interactions also show similarity in their contributions (18.4% and 17.8 %). S···S proportion is minimal to 1.6 % in thiophenol while the corresponding Se···Se proportion is 1.5 %. Thus, these structures obey the 'conservation of analogous interaction proportions' which we recently demonstrated in a series of chemical analogues of the antidepressant fenobam[25] (for details, see ESI). Further, interaction energies of the molecular dimers formed by each of these interactions were calculated using a molecular wave function based method reported recently.[26] Based on the values of pairwise intermolecular interaction energies, the topology interactions are represented using 'energy frameworks' (graphical representations where the radius of the beam connecting any two molecules is proportional to their interaction energy[27]). Interestingly, energy frameworks for thiophenol and selenophenol appear to be virtually identical (Fig 4). This is quite significant as it points to the similarity in corresponding interaction motifs in these compounds. In addition, it is possible to visualize the electrostatic and dispersion components in terms of energy frameworks, and it is found that the dispersion components predominate in the crystal packing of these compounds. Analysis of pairwise interaction energies show the strength hierarchy of interaction motifs in thiophenol as : dimer I(S–H···S,C–H···π/ -18.4 kJ/mol) > dimer II(C–H···π/ -14 kJ/mol) > dimers III-VI(non-directional/4-8 kJ/mol) > dimer VII (S–H···H–S/ -2.4 kJ/mol) > dimer VIII (S···S/ -0.6 kJ/mol) (figures of the dimers and electrostatic, dispersion and repulsion components of the energy values are given in ESI). Similarly, the interaction energy order in selenophenol is: dimer I(Se–H···Se,C–H···π/ -17.5 kJ/mol) > dimer II(C–H···π/ -14.2 kJ/mol) > dimers III-VI(non-directional/4-10 kJ/mol) > dimer VII (Se–H···H–Se/ -6.1 kJ/mol) > dimer VIII (Se···Se/ -3.2 kJ/mol).

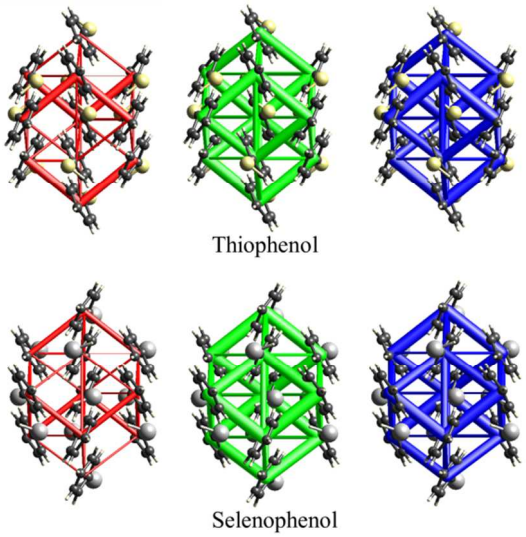

Fig 4. Isostructurality of thiophenol and selenophenol manifested in their energy frameworks (viewed down *c*-axis). Red, green and blue frameworks correspond to electrostatic, dispersion and total energy contributions.

It may be noted that in both structures dimers III-VI are formed by non-directional intermolecular forces which mainly originate from dispersion. Besides the one-to-one correspondence of analogous interaction motifs in thiophenol and selenophenol, their binding strengths also match to a great degree. And that explains the molecular origin of the formation of their solid solutions. In addition, the interaction energy estimations provides insights into the physical existence of thiophenol and selenophenol as liquids, and a likely rationale for the observed trends in their melting points in comparsion to phenol as: phenol (40 °C) > thiophenol (-15 °C) > selenophenol (-23 °C). Notably, the melting points of the selenophenol: thiophenol alloy phases were found to be -15.6 °C (1:9 phase) and -17.4 °C (3:1 phase). The fact that these mixed phases exhibit sharp endothermic peaks of melting in their DSC thermograms further confirms their alloy nature (See Fig S3 in ESI).

Further, theoretical charge density models were obtained based on single point periodic quantum mechanical calculations at the B3LYP/TZVP level using the positional parameters obtained from the single crystal X-ray analysis. Electron density topological analysis shows bond critical points (bcp) corresponding to the very rare varieties of S–H···S and Se–H···Se hydrogen bonds and S···S and Se···Se interactions.[28] The values of electron density (ρ_{bcp}) and its Laplacian ($\nabla^2\rho_{bcp}$) for S···S region in thiophenol are similar to those we recently reported for S···S interactions in an organic conductor.[16]

Table 2. Charge density topological features of intermolecular interactions in thiophenol and selenophenol. Values of kinetic energy density (G) and potential energy density (V) are given in (kJmol^{-1}bohr^{-3}).

Interaction	R_{ij}(Å)	ρ (eÅ^{-3})	$\nabla^2\rho$ (eÅ^{-5})	G	V	G/|V|
Thiophenol						
S–H···S	3.1078	0.02	0.4	7.7	-4.5	0.6
S···S	3.5837	0.07	0.6	14.6	-12.9	0.9
Selenophenol						
Se–H···Se	3.0830	0.03	0.5	10.0	-6.34	0.6
Se···Se	3.7562	0.05	0.5	11.2	-8.77	0.8
Alloy phase						
S–H···Se	2.9060	0.06	0.12	5.04	-6.82	0.7
Se–H···S	3.0882	0.04	0.09	3.09	-3.73	0.8
S···Se	3.5125	0.04	0.12	3.63	-4.01	0.9

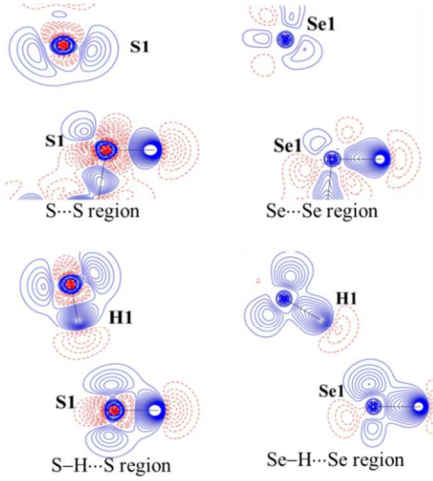

Fig 5. Static deformation density maps plotted with a contour level of ±0.05 eÅ^{-3} for thiophenol and selenophenol.

Similarly, ρ_{bcp} and $\nabla^2\rho_{bcp}$ values of Se···Se interaction in selenophenol are comparable to the values reported by Espinosa and co-workers based on experimental charge density.[15] It may be noted from the deformation density maps that lone pair electron densities on S and Se atoms are not oriented to favour effective homo-chalcogen interactions (Fig 5). While in an effective chalcogen bonding situation the valence shell charge concentration (CC) region is oriented towards charge depletion (CD) region forming effective CC-CD interaction, in the present cases of S···S and Se···Se interactions, the CC regions are oriented such that lone pair-lone pair repulsion is less. This feature is evident in the Laplacian maps (ESI). These charge density features rationalize the low degree of van der Waals sphere interpenetrations observed in S···S and Se···Se interaction regions. In contrast, in the S–H···S and Se–H···Se regions, the valance charge density distributions around S and Se atoms are quite in favour of the formation of hydrogen bonds, as seen in Fig 5. Charge density distribution indicates the CC-CD nature of this weakest class of hydrogen bonds, as it is the case with classical hydrogen bonds. Clearly, the CC regions corresponding to lone pairs on chalcogen atoms (classically, as in 'sp^3 hybridized' S and Se atoms) are oriented towards CD regions around the S–H/ Se–H protons. This is also obvious from corresponding Laplacian maps. The interaction energies of S–H···S and Se–H···Se hydrogen bonds are found to be -2.3 and -3.2 kJ/mol respectively (estimated from the charge density ρ_{bcp} and $\nabla^2\rho_{bcp}$ values, using Abramov's expression[29]). Hence, these hydrogen bonds need to be regarded among the weakest classes of hydrogen bonds, weaker than even C–H···O hydrogen bonds,[30] in terms of charge density distribution. Further, the electron density features of the Se···S, S–H···Se and Se–H···S interactions have also been calculated with their probable geometries in the alloy phase, and with the interaction distances obtained from the 43:57 alloy phase (Table 2).[31]

In summary, the solid phase isostructurality of thiophenol and selenophenol have been unravelled by *in situ* cryocrystallography and based on the similarity in intermolecular interactions, their solid solutions have been obtained. Systematic variations of cell parameters of these alloy phases resemble the Vegard's law-like behavior, a rare observation in organic solids. Our study further confirms the ability of organo sulfur and selenium to involve in virtually identical type of intermolecular interactions, notably the infinite S–H···S and Se–H···Se hydrogen bond chains and S···S and Se···Se contacts. Besides, the very weak nature of S···S and

Se···Se homo-chalcogen interactions and S–H···S, Se–H···Se hydrogen bonds have been unravelled by quantitative analysis of these crystal structures. In addition, the interaction energy estimations have provided insights into the trends in the melting points of the three phenols.

SPT thanks Prof Mark Spackman for the access to *CrystalExplorer (energy framework analysis)*. TNG Thanks DST, India for a JC Bose fellowship.

Notes and references

[a] *Solid state and Structural Chemistry Unit, Indian Institute of Science, Bangalore, India, 560012 E-mail: ssctng@sscu.iisc.ernet.in*
[b] *School of Chemistry and Biochemistry, The University of Western Australia, Crawley, WA 6009, Australia. Tel: +6164883151; E-mail: sajesh.thomas@uwa.edu.au*

† Electronic Supplementary Information (ESI) available: Deatails of crystallograhic refinement, energy framework calculations and theoretical charge density analysis. See DOI: 10.1039/b000000x/

1. G. R. Desiraju, *J Am Chem Soc*, 2013, **135**, 9952; G. R. Desiraju, *J Am Chem Soc*, 2013, **135**, 9952; G. R. Desiraju, J. J. Vittal and A. Ramanan, *Crystal Engineering: A Textbook*, World Scientific, 2011.
2. P. Vishweshwar, J. A. McMahon, J. A. Bis and M. J. Zaworotko, *J Pharm Sci-Us*, 2006, **95**, 499.
3. O. Bolton and A. J. Matzger, *Angew. Chem.*, 2011, **50**, 8960; K. B. Landenberger, O. Bolton and A. J. Matzger, *J Am Chem Soc*, 2015.
4. G. R. Desiraju, *Angew Chem Int Edit*, 1995, **34**, 2311; C. B. Aakeroy and D. J. Salmon, *Crystengcomm*, 2005, **7**, 439.
5. X. Xu, T. Xiao, X. Gu, X. Yang, S. V. Kershaw, N. Zhao, J. Xu and Q. Miao, *ACS Applied Materials & Interfaces*, 2015; X. Xu, B. Shan, S. Kalytchuk, M. Xie, S. Yang, D. Liu, S. V. Kershaw and Q. Miao, *Chem Commun*, 2014, **50**, 12828.
6. S. Etemad, E. M. Engler, T. D. Schultz, T. Penney and B. A. Scott, *Physical Review B*, 1978, **17**, 513; E. M. Engler, B. A. Scott, S. Etemad, T. Penney and V. V. Patel, *J Am Chem Soc*, 1977, **99**, 5909; Y. Shao and Y. Yang, *Advanced Functional Materials*, 2005, **15**, 1781.
7. A. I. Kitaigorodsky, Mixed Crystals, Springer, Berlin, 1984
8. M. Dabros, P. R. Emery and V. R. Thalladi, *Angewandte Chemie*, 2007, **119**, 4210.
9. D. S. Reddy, D. C. Craig and G. R. Desiraju, *J. Chem. Soc. Chem. Comm.*, 1994, 1457.
10. K. Sada, K. Inoue, T. Tanaka, A. Epergyes, A. Tanaka, N. Tohnai, A. Matsumoto and M. Miyata, *Angewandte Chemie*, 2005, **117**, 7221.
11. T. Jacobs, M. W. Bredenkamp, P. H. Neethling, E. G. Rohwer and L. J. Barbour, *Chem Commun*, 2010, **46**, 8341.
12. T. Hasell, S. Y. Chong, M. Schmidtmann, D. J. Adams and A. I. Cooper, *Angew. Chem.*, 2012, **51**, 7154; R. Natarajan, G. Magro, L. N. Bridgland, A. Sirikulkajorn, S. Narayanan, L. E. Ryan, M. F. Haddow, A. G. Orpen, J. P. H. Charmant, A. J. Hudson and A. P. Davis, *Angew. Chem.*, 2011, **50**, 11386; T. Fukushima, S. Horike, Y. Inubushi, K. Nakagawa, Y. Kubota, M. Takata and S. Kitagawa, *Angew. Chem.*, 2010, **49**, 4820; L. Travaglini, L. N. Bridgland and A. P. Davis, *Chem Commun*, 2014, **50**, 4803.
13. P. Metrangolo, F. Meyer, T. Pilati, G. Resnati and G. Terraneo, *Angew. Chem. Int. Ed.*, 2008, **47**, 6114; P. Metrangolo, H. Neukirch, T. Pilati and G. Resnati, *Acc Chem Res*, 2005, **38**, 386.
14. S. P. Thomas, K. Satheeshkumar, G. Mugesh and T. N. Guru Row, *Chem. Eur. J.*, 2015, 10.1002/chem.201405998.
15. M. E. Brezgunova, J. Lieffrig, E. Aubert, S. Dahaoui, P. Fertey, S. Lebegue, J. G. Angyan, M. Fourmigue and E. Espinosa, *Cryst Growth Des*, 2013, **13**, 3283.
16. M. Bai, S. P. Thomas, R. Kottokkaran, S. K. Nayak, P. C. Ramamurthy and T. N. Guru Row, *Cryst Growth Des*, 2013, **14**, 459.
17. S. Scheiner, *Acc Chem Res*, 2013, **46**, 280; S. Sarkar, M. S. Pavan and T. N. Guru Row, *Phys Chem Chem Phys*, 2015, **17**, 2330.
18. S. P. Thomas, M. S. Pavan and T. N. Guru Row, *Chem Commun (Camb)*, 2014, **50**, 49.
19. V. E. Zavodnik, V. K. Bel'skii and P. M. Zorkii, *Zh. Strukt.Khim.*, 1987, **28**.
20. D. R. Allan, S. J. Clark, A. Dawson, P. A. McGregor and S. Parsons, *Acta Cryst. B*, 2002, **58**, 1018.
21. R. Desiraju Gautam, P. S. Ho, L. Kloo, C. Legon Anthony, R. Marquardt, P. Metrangolo, P. Politzer, G. Resnati and K. Rissanen, in *Pure Appl. Chem*, 2013, vol. 85, p. 1711.
22. (a) L. Vegard, Z. Phys., 1921, 5, 17. (b) L. Vegard, Z. Cryst., 1928, 67, 239.
23. S. P. Thomas, S. P. K. P. Veccham, L. J. Farrugia and T. N. G. Row, *Cryst. Growth Des.*, 2015, 10.1021/cg5016687.
24. J. J. McKinnon, D. Jayatilaka and M. A. Spackman, *Chem Commun*, 2007, 3814; M. A. Spackman and D. Jayatilaka, *Crystengcomm*, 2009, **11**, 19.
25. S. P. Thomas, K. Nagarajan and T. N. G. Row, *Chem Commun*, 2012, **48**, 10559; S. P. Thomas, K. Shashiprabha, K. R. Vinutha, S. P. Nayak, K. Nagarajan and T. N. G. Row, *Cryst Growth Des*, 2014, **14**, 3758.
26. M. J. Turner, S. Grabowsky, D. Jayatilaka and M. A. Spackman, *J. Phys. Chem. Lett.*, 2014, **5**, 4249.
27. M. J. Turner, S. P. Thomas, M. W. Shi, D. Jayatilaka and M. A. Spackman, *Chem Commun*, 2015, **51**, 3735.
28. Crystal Structure Databse shows only 4 examples of Se-H...Se hydrogen bonds (CCDC codes: HUCJUL, HUDBUE, NUVVOQ, YERJAG).
29. E. Espinosa and E. Molins, *J Chem Phys*, 2000, **113**, 5686; Y. A. Abramov, *Acta Cryst. A*, 1997, **53**, 264.
30. U. Koch and P. L. A. Popelier, *J. Phys. Chem.*, 1995, **99**, 9747; P. Munshi and T. N. Guru Row, *J. Phys. Chem. A*, 2005, **109**, 659; S. P. Thomas, M. S. Pavan and T. N. G. Row, *Cryst Growth Des*, 2012, **12**, 6083.
31. The crystal structure of 43:57 phase is supposed to be representing a crude, average picture of the selenophenol-thiophenol interactions. The calculations were performed at B3LYP/6-311++G(d,p) level.